

# INVESTIGATION OF NEAR-SURFACE HYDROGEN IN CAVITY-GRADE NIOBIUM

A. Romanenko\*, Fermilab, Batavia, IL 60510, USA

L.V. Goncharova, The University of Western Ontario, London, ON, Canada

## Abstract

Details of the distribution of near-surface hydrogen in niobium cavities are important for research into possible mechanisms involving hydrogen, which affect the dependence of the cavity quality on the magnitude of surface fields. We utilized an elastic recoil detection (ERD) technique with the depth resolution of about one nanometer on samples, which underwent different treatments similar to the ones with the known effect on cavity performance. Results of the study indicate a significant segregation of hydrogen within the first few nanometers near the surface. Standard heat treatments, such as 600°C, 800°C and 120°C heat treatments, do not systematically change the near-surface hydrogen content.

## INTRODUCTION

Recent developments in the research on the high field Q-slope and mild baking effect highlighted the need to understand in detail the distribution of hydrogen in niobium.

Superconducting RF (SRF) cavities made of bulk niobium are used as primary accelerating structures in a number of present and future accelerators based on the superconducting technology. Significant progress has been made in the last few years in achieving better accelerating gradients in SRF cavities. Nevertheless, full understanding of surface structure of niobium used in cavities is not yet developed. One area of recent active research is the contributions of different near-surface lattice defects to the cavity performance at high fields, and in particular on a *high field Q-slope* (HFQS) (see [1] for review). An underlying mechanism of a strong effect of the in situ vacuum baking at 120°C for 48 hours on the high field performance of niobium cavities remains controversial.

A key question is what particular material intrinsic or extrinsic properties are leading to the RF losses in the HFQS. A closely related and equally important question is what changes in the niobium near-surface composition and structure at 120°C. Several niobium defects, such as dislocations [2], vacancies [3], and near-surface interstitial hydrogen [4] are currently considered as possible causes of the HFQS and all can be active in the experimentally observed mild baking effect. For all three types of defects, it is crucial to understand their distribution and change on the scale of magnetic field penetration depth (about 40 nm) during cavity processing treatments. In particular, for dislocations and vacancies, hydrogen may be involved in the mild bak-

ing effect via vacancy-hydrogen complexes [5], while the interstitial hydrogen model relies on the changes of hydrogen content itself during different treatments. An earlier study [6] explored the effect of different chemical etching solutions on the near-surface hydrogen content with the depth resolution limited at the time to about 30 nm due to the detection method. In this study we advance the hydrogen distribution issue by using ERD on samples treated using different thermal and chemical etching steps with known outcomes on RF cavities. Additionally ERD spectra of two cavity cutout samples were measured and correlated with their drastically different RF behavior.

## EXPERIMENTAL

### *Samples Preparation and RF Tests*

We used two types of samples for the studies: (i) rectangular 1.2×1.5 cm, 3 mm thick samples cut with wire electrical discharge machining (EDM) from RRR 300 single grain niobium sheet and subjected to 150 μm buffered chemical polishing after cutting; (ii) circular cutouts from a large grain buffered chemical polished (BCP) cavity limited by the HFQS and a fine grain electro polished (EP) cavity free of the HFQS.

Niobium sheet samples were subjected to a sequence of surface treatments similar to those performed on cavities with the known outcomes on RF performance. Several different surface treatments were tried including (i) vacuum baking at 600°C for 10 hours, (ii) 800°C for 4 hours, (iii) 120°C for 48 hours, and (iv) rinsing in a concentrated (48%) hydrofluoric acid (HF) for 20 minutes. Details of the treatments with the list of samples used in the studies are shown in Table 1. Cavity cutout samples come from two different cavities: large grain BCP cavity LE1-37 with the grain size of about 10 cm, and a fine grain TE1AES004 EP cavity with the grain size of about 50 μm. TE1AES004 was subjected to 120°C 48 hours vacuum treatment to eliminate the HFQS. LE1-37 cavity was limited by the HFQS and the cutout represents an area with high RF losses in the HFQS regime (hot spot). Details on LE1-37 cavity tests and surface analytical techniques applied on cutouts are reported elsewhere [5, 7, 8]. TE1AES004 cutout represents an area without any RF losses (cold spot) up to the highest field reached, which was determined by the localized quench at a different location. Full analysis of other TE1AES004 cutouts using alternative techniques is currently underway and will be published elsewhere. Temperature increase of the outside cavity wall was registered with carbon resis-

\* aroman@fnal.gov

tance thermometers during RF test for both cutouts at each field level and the results are shown in Figure 1.

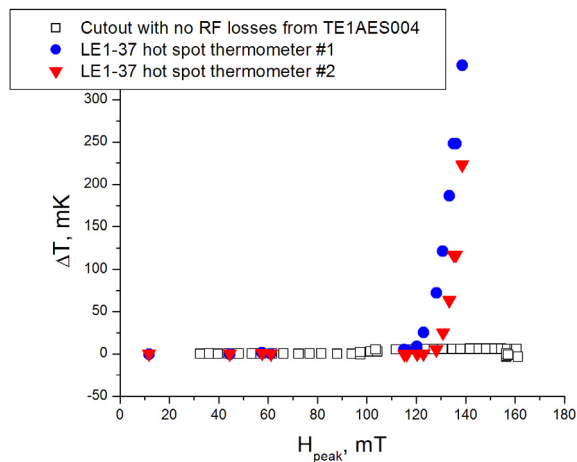


Figure 1: Temperature variations of the outside cavity walls in the cutout regions during RF tests at different magnetic field levels. LE1-37 cutout had two thermometers attached during RF test separated by about 1 cm, and both registered a strong HFQS heating starting from about 120 mT (solid red triangles and blue circles). TE1AES004 cutout (empty squares) exhibits no temperature increase up to the highest field.

### Hydrogen ERD Analysis

Niobium samples were studied using a 1.6 MeV  $^4\text{He}$  beam in a conventional ERD setup with incident angle of  $75^\circ$ , recoil angle of  $30^\circ$  in IBM geometry and  $6.1 \mu\text{m}$  Al-coated mylar range foil. In IBM geometry incident beam, exit beam and the surface normal are in the same plane [9]. Kapton and H-implanted Si targets were used as standards to determine the detector solid angle, both agreed at  $\sim 3\%$ . Charge collection was monitored by an intermittent Faraday cup that intercepts the beam in front of the target with a duty cycle (beam-on-target fraction) of  $\sim 75\%$ . An HF-etched Si sample exposed to air for a short period of time was analyzed to estimate possible surface hydrocarbon contamination. Note that all ERDA data represent averages over a sample area ( $2\text{-}10 \text{ mm}^2$ ); this makes it difficult for us to distinguish between a near-interface compositional gradient and interface or surface roughness [10, 11].

Measurements were performed at multiple spots on each sample separated by at least 1-2 mm, and typical spot-to-spot variation is shown in Figure 2 on the example of sample HA-4. The spot-to-spot variation is below 5% (as calculated from integrated near-surface intensity for the channels within the 375-480 keV energy window), suggesting a uniform distribution of hydrogen over the sample surface. Similar results were obtained on all other investigated samples.

SIMNRA, v. 6.05 [9] was used to fit experimental data

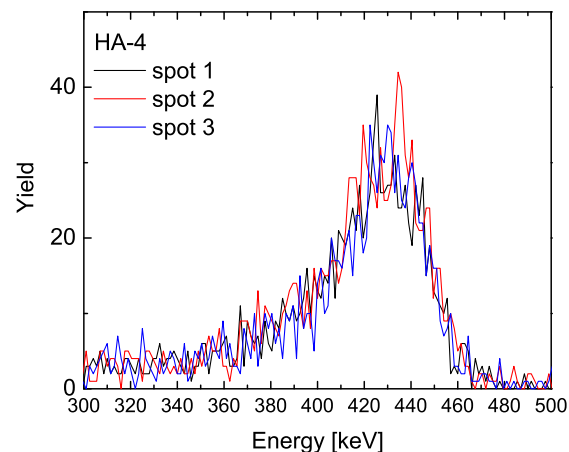


Figure 2: Spot-to-spot variation of elastic recoil spectra for HA-4 sample. Other samples exhibited similar low variation.

in order to extract the depth profiles of hydrogen concentration. We assume the surface composition of bulk niobium as shown in Figure 3, which is a generally accepted structure deduced by surface analytical techniques such as TEM, XPS, AES, and SIMS. Several assumptions were

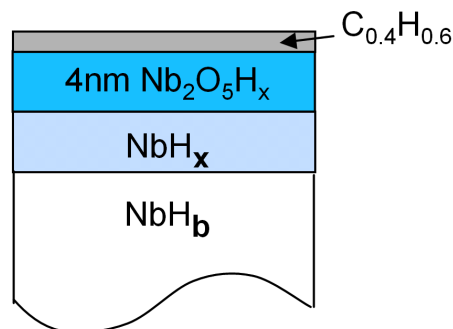


Figure 3: Surface structure of Nb assumed for ERD data fitting.

made for fitting the data in order to obtain the depth distribution of hydrogen.

In particular, total hydrogen yield in experimental ERDA spectra was reduced by H atomic density of  $6 \times 10^{15} \text{ at/cm}^2$ . This amount is roughly equivalent to the 10-12 Å thick layer of hydrocarbons ( $\text{C}_{0.4}\text{H}_{0.6}$ ) or alternative hydrogen containing molecules giving raise to additional hydrogen yield from the surface. Calculated hydrogen peak intensity corresponding to this hydrogen atomic density was subtracted from the experimental intensity for samples HA1-6.

The surface layer of 4 nm thick  $\text{Nb}_2\text{O}_5$  (density =  $4.47 \text{ g/cm}^3$ ) was assumed. Bulk Nb density ( $8.7 \text{ g/cm}^3$ ) was used for the deepest  $\text{NbH}_b$  layer, and interfacial  $\text{NbH}_x$

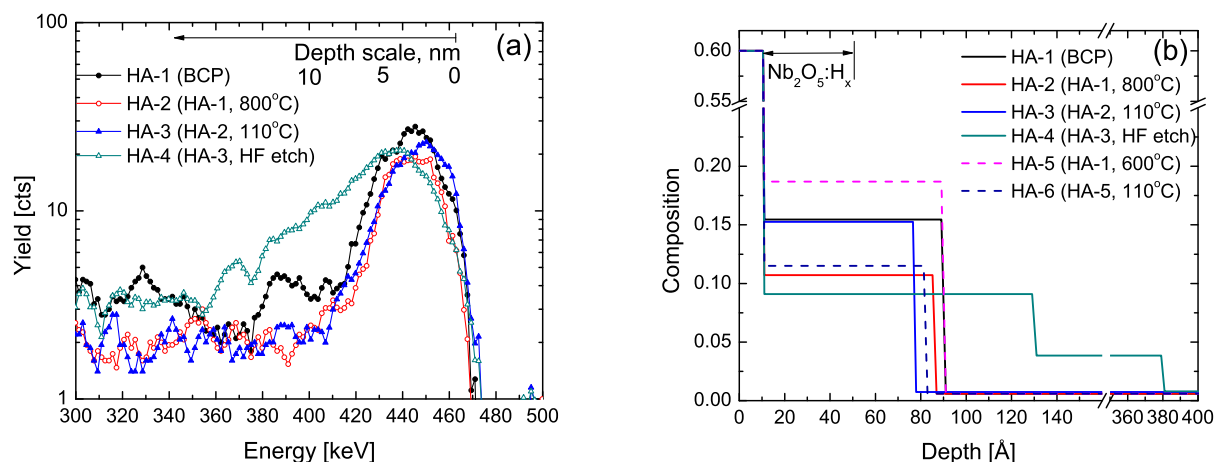


Figure 4: Experimental data (a) and the depth profile of hydrogen atomic concentration obtained by fitting the data (b).

layer density of  $7.72 \text{ g/cm}^3$  was applied for thickness calculations (assuming roughly 10% hydrogen content).

### Results on Nb Sheet Samples

The summary of the ERDA results for niobium sheet samples is presented in Figure 4. Note that only four samples are shown for clarity. The observed hydrogen distributions reveal the near-surface segregation in all samples within the first few nanometers while the bulk hydrogen content is below 1 atomic percent and does not vary dramatically between the samples. Note that ERDA detection limit is on the order of 20 at.ppm. A hydrogen enriched layer is about 8-9 nm thick for all samples (except HA-4), which includes 4 nm of  $Nb_2O_5$  used for the best fit as described above. Comparison hydrogen profiles (Figure 4) for samples HA-1, HA-2, and HA-3 indicates that hydrogen content is reduced after consecutive heat and chemical treatments. Hydrogen depth distribution is significantly different for the HA-4 sample, which was rinsed in HF for 20 minutes following the  $800^\circ\text{C}$  4 hours and  $120^\circ\text{C}$  74 hours high temperature treatments. In HA-4 sample hydrogen enrichment is extending to about 40 nm deep with hydrogen gradient slowly decreasing into Nb bulk (as shown schematically by two layers of different hydrogen content in the right panel of Figure 4). Note that hydrogen concentration in the near surface region is lower in sample HA-4 compared to other samples.

### Results on Cavity Cutouts

If the near-surface hydrogen is the primary cause of the observed difference in RF behavior of the cavity cutouts (Figure 1), we would expect to observe a difference in hydrogen depth profiles. However we observe exactly the same hydrogen distributions in both device cutouts as shown in Figure 5, along with the typical spot-to-spot vari-

ation shown for the TE1AES004 cutout.

ERDA results and calculated depth profiles show hydrogen enrichment for cavity cutouts, but the depth of the enriched layer is shorter than in the niobium sheet samples. The concentration of hydrogen at the niobium oxide/niobium interface is about 16 at.%, which is comparable to the niobium sheet samples.

## DISCUSSION

One of the possible causes for the HFQS and its sensitivity to different treatments may be due to differences in near-surface hydrogen content. There is some correlation reported between the cavity performance and the concentration of hydrogen from secondary ion mass spectrometry (SIMS) measurements on control samples treated with the cavity [4]. But the quantification of profiles in SIMS is a challenge due to the matrix effects and uncertainty of ionization yields at the interfaces. Our results do not support the correlation between the concentration of hydrogen in the near-surface layer and cavity performance. The most significant result is almost exactly the same hydrogen depth profile in cutout samples coming from large grain BCP cavity hot spot and a fine grain EP cavity cold spot. (Local heating registered at these locations during respective cavity tests is drastically different - a strong HFQS heating up to a few hundred mK in one case starting from about 100 mT, and no registered heating at all in the other case up to 160 mT.) This result suggests that variation of hydrogen concentration is likely not the cause of the difference. But, since ERD does not distinguish between hydrogen in the interstitials or precipitates, it may be possible that the difference in losses comes from different precipitation states in these two samples rather than different amount of hydrogen dissolved in the lattice. Furthermore, hydrogen can still be involved indirectly in the mild baking effect via

Table 1: Hydrogen profiling results. Quantitative fittings of hydrogen distribution are obtained based on the niobium surface layer model from Fig. 3, with  $x$ ,  $y$ ,  $b$  corresponding to the fraction of hydrogen in, respectively, oxide, near-surface layer, and bulk niobium.

Sample	Treatment	Enriched layer, nm	$x$	$y$	$b$
HA-1	BCP 150 $\mu\text{m}$	4	0.15	0.15	0.008
HA-2	BCP 150 $\mu\text{m}$ + 800°C 4 hours	3.6	0.11	0.11	0.006
HA-3	BCP 150 $\mu\text{m}$ + 800°C 4 hours + 110°C 74 hours	2.7	0.15	0.15	0.008
HA-4	BCP 150 $\mu\text{m}$ + 800°C 4 hours + 110°C 74 hours + HF rinsing 20 mins	8/25	0.09	0.09/0.04	0.008
HA-5	BCP 150 $\mu\text{m}$ + 600°C 10 hours	4	0.19	0.19	0.006
HA-6	BCP 150 $\mu\text{m}$ + 600°C 10 hours + 110°C 54 hours	4	0.11	0.11	0.006
LE1-37 hot spot	BCP 200 $\mu\text{m}$	0.7	0.16	0.16	0.006
TE1AES004 cold spot	EP 120 $\mu\text{m}$ + 120°C 48 hours	0.7	0.16	0.16	0.006

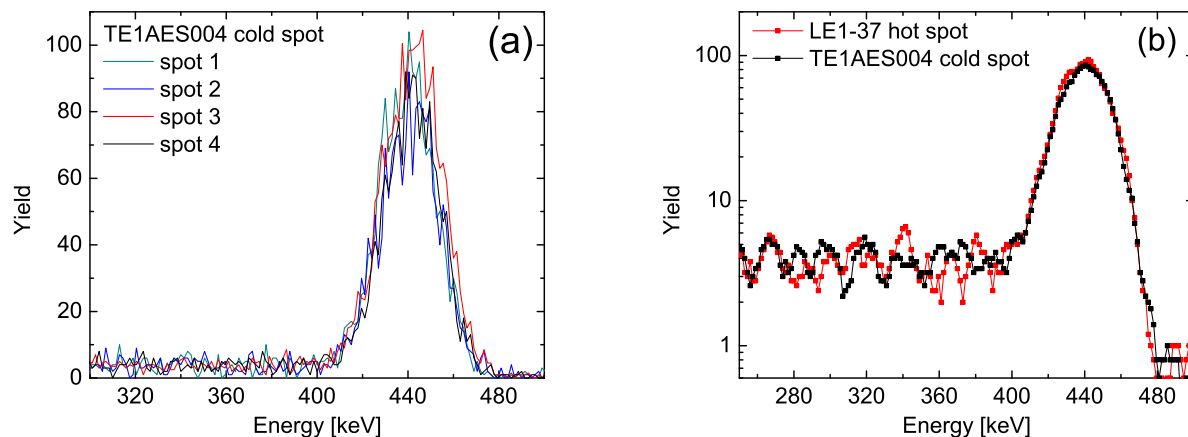


Figure 5: Spot-to-spot variation of ERD spectra (a) and raw data on LE1-37 and TE1AES004 cavity cutouts (b). Both spectra are strikingly similar even though they come from completely different cavities exhibiting drastically different RF losses with field.

vacancy-hydrogen complexes dissociation resulting in the free vacancy mobility.

Another result is a significant near-surface hydrogen segregation in all samples. The absolute atomic concentration of H in Nb lattice is very high and ranges from 9 to 19 atomic %. Such a high hydrogen content should lead to the abundance of hydrogen-induced lattice defects such as vacancy-hydrogen complexes [12]. If the ordered hydride phases are precipitated, misfit dislocations are also possible [13], which may account for possible differences

between surface and bulk dislocation densities. In addition, this level of hydrogen corresponds to the mixed  $\alpha + \beta$  phase at room temperature in the phase diagram from [14]. This finding indicates that precipitates of  $\beta$ -phase may be present in the surface layer of all niobium cavities independent of the standard heat treatments chosen if nucleation sites exist for precipitates to form. The recent discovery of dendritic hydrides in lossy areas of cavity walls at high magnetic fields [15] confirms this conclusion.

Systematic studies following the cavity surface treatment

path show that H concentration in the first few nanometers does not change significantly during heat treatments and does change after HF rinsing resulting in the hydrogen-rich layer extending to a greater depth. We speculate that this effect might be caused by the removal of the natural oxide layer during HF rinsing, which normally serves as a barrier for additional hydrogen adsorption.

Finally we note that niobium sheet samples used for the studies did not go through severe mechanical deformation as in the case of cavity deep drawing used to form half-cells from niobium sheets. In principle, the mobility of hydrogen during heat treatments should be affected by the presence of dislocations and vacancies, which serve as hydrogen trapping sites. Hence we intend in future work to perform similar studies along the cavity processing steps with samples pre-deformed to a different degree and cavity cutouts subjected to further heat and chemical treatments.

## CONCLUSION

Using elastic recoil detection technique on niobium sheet samples subjected to different treatments along SRF cavity processing steps, we demonstrate a near-surface hydrogen enrichment, which is not removed by 800°C, 600°C and 120°C heat treatments typically applied to cavities. The level of hydrogen in the near-surface region indicates the possible room temperature presence of both  $\alpha$  and  $\beta$  phases as well as the possibility of hydrogen-induced lattice defects such as vacancies and dislocations. A comparison between cavity cutouts exhibiting drastically different RF behavior shows the same hydrogen depth profile indicating that if hydrogen is involved then a different degree of precipitation for the same total amount of hydrogen may be the real reason behind the difference in RF losses.

## ACKNOWLEDGEMENTS

We would like to acknowledge valuable discussions with L. Cooley and G. Wu from Fermilab, A. Grassellino from TRIUMF, and H. Padamsee from Cornell University. We thank Gianluigi Ciovati from Jefferson Lab for TE1AES004 EP cavity test with thermometry, and Jack Hendriks of the Western Tandatron Accelerator Facility for valuable help with ion beam analysis.

## REFERENCES

- [1] H. Padamsee. *RF Superconductivity: Volume II: Science, Technology and Applications*. Wiley-VCH, 2009.
- [2] A Romanenko and H Padamsee. The role of near-surface dislocations in the high magnetic field performance of superconducting niobium cavities. *Superconductor Science and Technology*, 23(4):045008, 2010.
- [3] B. Visentin, M. F. Barthe, V. Moineau, and P. Desgardin. Involvement of hydrogen-vacancy complexes in the baking effect of niobium cavities. *Phys. Rev. ST Accel. Beams*, 13(5):052002, May 2010.
- [4] G. Ciovati, G. Myneni, F. Stevie, P. Maheshwari, and D. Griffiths. High field  $q$  slope and the baking effect: Review of recent experimental results and new data on nb heat treatments. *Phys. Rev. ST Accel. Beams*, 13(2):022002, Feb 2010.
- [5] A. Romanenko. *Surface characterization of niobium cavity sections: understanding the high field Q-slope*. PhD thesis, Cornell University, 2009.
- [6] C. Z. Antoine, B. Aune, B. Bonin, J.M. Cavedon, M. Juillard, A. Godin, C. Henriot, P. Leconte, H. Safa, A. Veysièrre, A. Chevarier, and B. Roux. The role of atomic hydrogen in q-degradation of niobium superconducting rf cavities: analytical point of view. In *Proceedings of the Fifth Workshop on RF Superconductivity, DESY, Hamburg, Germany*, pages 616–634, 1991.
- [7] A. Romanenko, H. Padamsee, G. Ereemeev, and J. Shu. Comparative surface studies on fine-grain and single crystal niobium using XPS, AES, EBSD and profilometry. In *Proceedings of PAC2007*, 2007.
- [8] A. Romanenko. Crystalline microstructure role in the high-field Q-slope. In *Proceedings of 14th International Conference on RF Superconductivity*, 2009.
- [9] M. Mayer. SIMNRA user's guide. IPP 9/113, Max-Planck-Institut für Plasmaphysik, Garching, Germany, 1997.
- [10] S. L. Molodtsov, A. F. Gurbich, and C. Jeynes. *J. Phys. D: Appl. Phys.*, 41:205303, 2008.
- [11] W. H. Schulte, B. W. Busch, E. Garfunkel, T. Gustafsson, G. Schiwietz, and P. L. Grande. *NIMB*, 183:16–24, 2001.
- [12] J. Cizek, I. Prochazka, R. Kuzel, F. Becvar, M. Cieslar, G. Brauer, W. Anwand, R. Kirchheim, and A. Pundt. Hydrogen-induced defects in niobium studied by positron annihilation spectroscopy. *J. of Alloys and Compounds*, 404–406:580–583, 2005.
- [13] B.J. Makenas and H.K. Birnbaum. Phase changes in the niobium-hydrogen system i: accommodation effects during hydride precipitation. *Acta Metallurgica*, 28:979–988, 1980.
- [14] F. D. Manchester and J. M. Pitre. *Phase Diagrams of Binary Hydrogen Alloys*. ASM International, 2000.
- [15] A. Romanenko, G. Wu, G. Ciovati, and L. D. Cooley. Post-baking losses in electropolished niobium cavities: dissection studies. In *Proceedings of the 15th International Conference on RF Superconductivity*, number ThPO08, 2011.